Available online at www.sciencedirect.com
ScienceDirect
Journal of Power Sources 175 (2008) 238–243
JOURNAL OF POWER SOURCES
www.elsevier.com/locate/jpowsour

Short communication

Performance of fuel cells with proton-conducting ceria-based composite electrolyte and nickel-based electrodes

Jianbing Huang, Zongqiang Mao *, Zhixiang Liu, Cheng Wang

Institute of Nuclear and New Energy Technology, Tsinghua University, Beijing 100084, China

Received 30 August 2007; received in revised form 11 September 2007; accepted 11 September 2007
Available online 14 September 2007

Abstract

A ceria-based composite electrolyte with the composition of $Ce_{0.8}Sm_{0.2}O_{1.9}$ (SDC)–30 wt.% ($2Li_2CO_3$:$1Na_2CO_3$) is developed for intermediate temperature fuel cells (ITFCs). Two kinds of SDC powders are used to prepare the composite electrolytes, which are synthesized by oxalate coprecipitation process and glycine–nitrate process, respectively, and denoted as SDC(OCP) and SDC(GNP). Based on each composite electrolyte, two single cells with the electrolyte thickness of 0.3 and 0.5 mm are fabricated by dry-pressing technique, using nickel oxide as anode and lithiated nickel oxide as cathode, respectively. With H_2 as fuel and air as oxidant, all the four cells exhibit excellent performances at 400–600 °C, which can be attributed to the highly ionic conducting electrolyte and the compatible electrodes. The cell performance is influenced by the SDC morphology and the electrolyte thickness. More interestingly, such composite electrolytes are found to be proton conductors at intermediate temperature range for the first time since almost all water is observed at the cathode side during fuel cell operation for all cases. The unusual transport property, excellent cell performance and potential low cost make this kind of composite material a good candidate electrolyte for future cost-effective ITFCs.

Keywords: Intermediate temperature fuel cells (ITFCs); Proton; $Ce_{0.8}Sm_{0.2}O_{1.9}$ (SDC); Carbonate; Composite electrolyte; Performance

1. Introduction

Solid-state fuel cells operated at intermediate temperatures (400–600 °C) have attracted much attention since they combine the advantages of high- and low-temperature fuel cells such as fast electrode kinetics, low material degradation and low cost for system construction. To develop high-performance intermediate temperature fuel cells (ITFCs), a solid electrolyte with high ionic conductivity is required. Most research efforts are focused on the oxide electrolytes, e.g. doped ceria [1], doped lanthanum gallate [2] and doped barium cerate [3]. These materials exhibit higher ionic conductivity at intermediate temperatures than the state-of-the-art yttria-stabilized zirconia (YSZ) for high-temperature solid oxide fuel cells (HTSOFCs). However, they must be prepared into a dense ceramic film as thin as 10 μm to achieve considerable cell output. There are still many problems with respect to thin-film preparation and material strength which are barriers to develop practical fuel cells for commercial applications.

In recent years novel ceria-based composite materials have been developed successfully as electrolytes for intermediate temperature fuel cells [4–10]. These materials show superionic conductivity of 10^{-2} to 1 S cm^{-1} at 400–600 °C [7]. Among these ceria-based composites, the ceria–carbonate composites are the most commonly used electrolyte materials, which have demonstrated the best performances in fuel cell application. It has been reported that the SDC–carbonate composites are hybrid O^{2-}/H^+ conductors, and the oxygen ion conduction is predominant over the proton conduction [11,12]. But in this study we fabricated single cells with typical SDC–carbonate composite electrolytes by dry-pressing technique and found that these composite materials are mainly proton conductors since almost all water was observed at the cathode side during fuel cell operation. Here we examine the effects of the SDC morphology and the electrolyte thickness on the cell performances, and discuss both the dc and ac conductivity behaviors of the composite electrolytes to reveal the conduction mechanism.

2. Experimental

$Ce_{0.8}Sm_{0.2}O_{1.9}$ (SDC) powders were synthesized by oxalate coprecipitation process and glycine–nitrate process,

* Corresponding author. Tel.: +86 10 62780537; fax: +86 10 62771150.
E-mail address: maozq@tsinghua.edu.cn (Z. Mao).

0378-7753/$ – see front matter © 2007 Elsevier B.V. All rights reserved.
doi:10.1016/j.jpowsour.2007.09.018

respectively. Precursor solution was achieved by dissolving $Ce(NO_3)_3{\cdot}6H_2O$ and Sm_2O_3 in dilute nitrate acid according to their stoichiometric proportion. In the oxalate coprecipitation process, oxalate precipitate was obtained by dripping the precursor solution to oxalic acid solution, which had been adjusted to neutral pH (6.6–6.9) by dilute ammonia solution. After fully washed by water and ethanol, the precipitate was calcined at 750 °C for 2 h to form the cubic fluorite structure. In the glycine–nitrate process, glycine was blended with the precursor solution in a ratio of 2. By heating the solution, autogeneous combustion occurred, and fine SDC 'ash' of pale-yellow in color sprayed out. The collected SDC 'ash' was calcined at 750 °C for 2 h to remove the carbon residues and to form a well-crystalline structure. The SDC powders synthesized by above two processes were denoted as SDC(OCP) and SDC(GNP), respectively. Then the two SDC powders were mixed with the binary carbonates separately according to the composition of SDC–30 wt.% ($2Li_2CO_3$:$1Na_2CO_3$) and heat-treated at 680 °C for 40 min. The resultants were taken directly from the furnace to room temperature and ground thoroughly for use as electrolyte materials.

Based on each SDC–carbonate composite electrolyte, two single cells were fabricated by dry-pressing technique. The composite anode was the mixture of nickel oxide (50 vol.%) and electrolyte (50 vol.%). The cathode powder was composed of lithiated nickel oxide (50 vol.%) mixed with electrolyte (50 vol.%). The anode, electrolyte and cathode were loaded orderly into a Φ 13 mm mold and co-pressed into a pellet at a pressure of 300 MPa and then sintered at 600 °C in air for 30 min. Two final thicknesses of the composite electrolyte layer, 0.3 and 0.5 mm, were obtained by controlling the composite amount. For each cell, the thicknesses of anode and cathode were 0.5 and 0.3 mm, respectively. The effective working area of the pellets was 0.785 cm^2. Both sides of the pellets were coated with silver paste to improve electrical contact. Stainless steel was employed as testing holder. Before measurement, two pieces of nickel foams were placed on both sides of the holder as current collectors. Then silver glue was applied as the sealant. To directly observe the water formed at each electrode side, each gas outlet of the testing holder was connected to a clear and dry conical flask with a long plastic tube. The cells were tested between 400 and 600 °C, using hydrogen as fuel and air as oxidant, respectively. Both gas flow rates were controlled between 40 and 100 mL min^{-1} under 1 atm pressure.

To confirm the phase structure and morphology of the SDC powders and SDC–carbonate composites, the powder XRD (D8 ADVANCE, Bruker AXS Corp. German) and SEM (JSM-6301F, JEOL Ltd., Japan) were performed. For ac conductivity measurement, the SDC powders and the SDC–carbonate composites were pressed uniaxially under 300 MPa to form pellets of 13 mm in diameter, and then sintered at 1350 °C for 4 h and 600 °C for 1 h, respectively. Silver electrodes were prepared by painting silver paste onto both sides of the pellets, and heated at 600 °C for 40 min. Electrical conductivity of the pellets was measured in air by two-probe impedance spectroscopy. The measurements were conducted with a Perkin-Elmer 5210 frequency response analyzer combined with EG&G PAR potentiostat/galvanostat 263 A. Impedance data were taken over a temperature range of 400–600 °C and a frequency range of 100 mHz to 100 kHz using an excitation voltage of 10 mV.

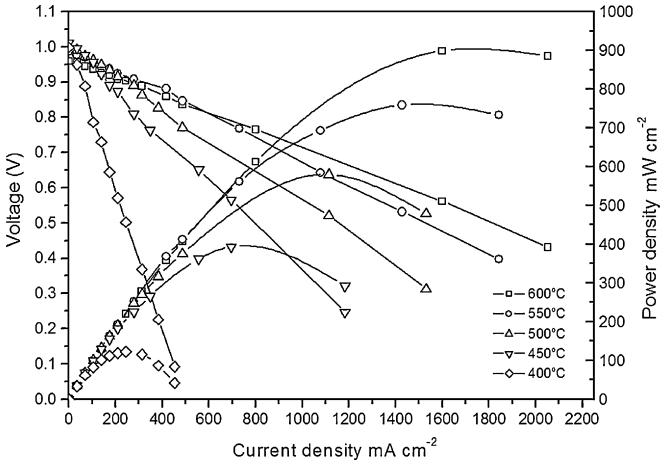

Fig. 1. *I–V* and *I–P* characteristics of a single cell with SDC(OCP)-based composite electrolyte (0.5 mm in thickness) at various temperatures.

3. Results and discussion

Four cells with SDC-based composite electrolyte and nickel-based electrodes were investigated at intermediate temperatures and the cell performances are shown in Figs. 1–4. For all the four cells, the open-circuit voltages (OCVs) exceed 0.94 V at 600 °C, and some reach 1.00 V or even higher value, e.g. 1.07 V in the case of thick electrolyte. While the OCV of the fuel cells with a SDC or GDC thin-film electrolyte is difficult to exceed 0.90 V at 600 °C due to the electronic conduction resulting from the reduction of Ce^{4+} to Ce^{3+} at H_2 atmosphere [13]. This indicates the electronic conduction of SDC can be suppressed effectively by the introduction of a certain amount of carbonates. However, the OCVs of single cells vary with the SDC morphology and the electrolyte thickness. According to

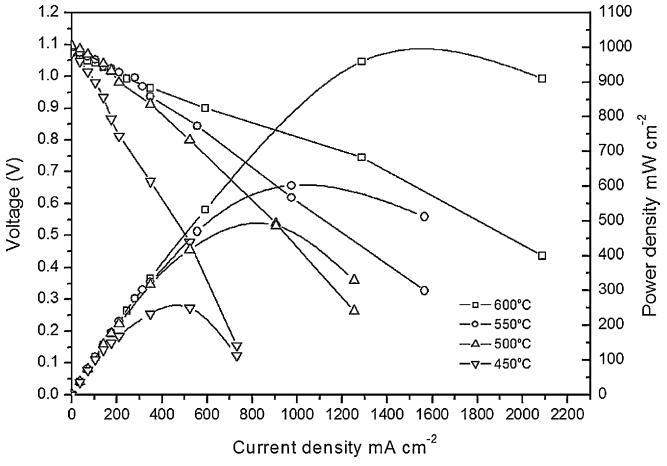

Fig. 2. *I–V* and *I–P* characteristics of a single cell with SDC(GNP)-based composite electrolyte (0.5 mm in thickness) at various temperatures.

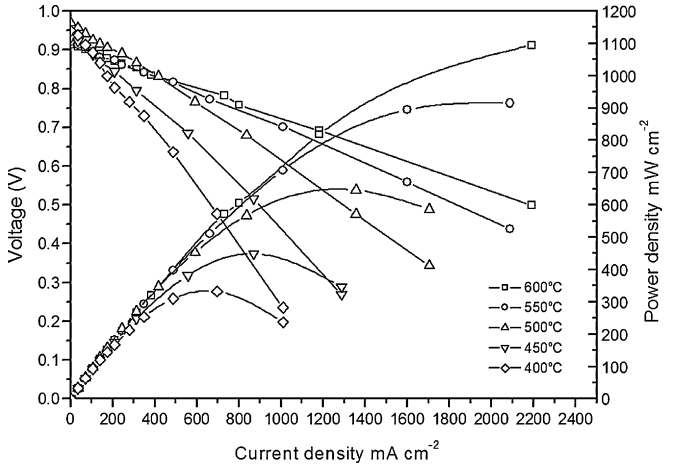

Fig. 3. *I–V* and *I–P* characteristics of a single cell with SDC(OCP)-based composite electrolyte (0.3 mm in thickness) at various temperatures.

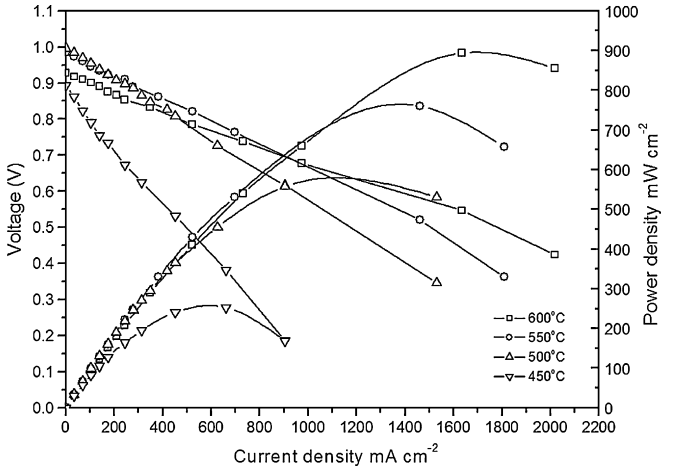

Fig. 4. *I–V* and *I–P* characteristics of a single cell with SDC(GNP)-based composite electrolyte (0.3 mm in thickness) at various temperatures.

Figs. 1–4, it is evident that in the case of the same composite electrolyte the fuel cells with a 0.5 mm thick electrolyte show higher OCVs than those with a 0.3 mm thick electrolyte. In the other hand, the cells with a SDC(GNP)-based composite electrolyte show higher OCVs than those with a SDC(OCP)-based composite electrolyte. This can be explained as a result of the difference in the density/porosity of composite electrolytes with different SDC phases.

As shown in Fig. 5(a) and (b), the morphology of the SDC(OCP) powder is distinct from that of the SDC(GNP) powder. The SDC(GNP) powder presents a highly porous foam-like structure, whereas the SDC(OCP) powder consists of flat plate-like particles. The low fill density of the foam powder makes it possible to fabricate dense electrolyte thin membrane with a simple dry-pressing process, which has been reported by Xia and Liu [14]. The SEM photos of the corresponding SDC–carbonate composites are shown in Fig. 5(c) and (d). It can find that in the SDC(OCP)-based composite the surfaces of the SDC particles are covered with amorphous carbonates to form an aggregate group with clear interfaces; while in the SDC(GNP)-based composite a homogenous composite bulk is formed without clear interfaces due to the reconstruction of the SDC particles after the

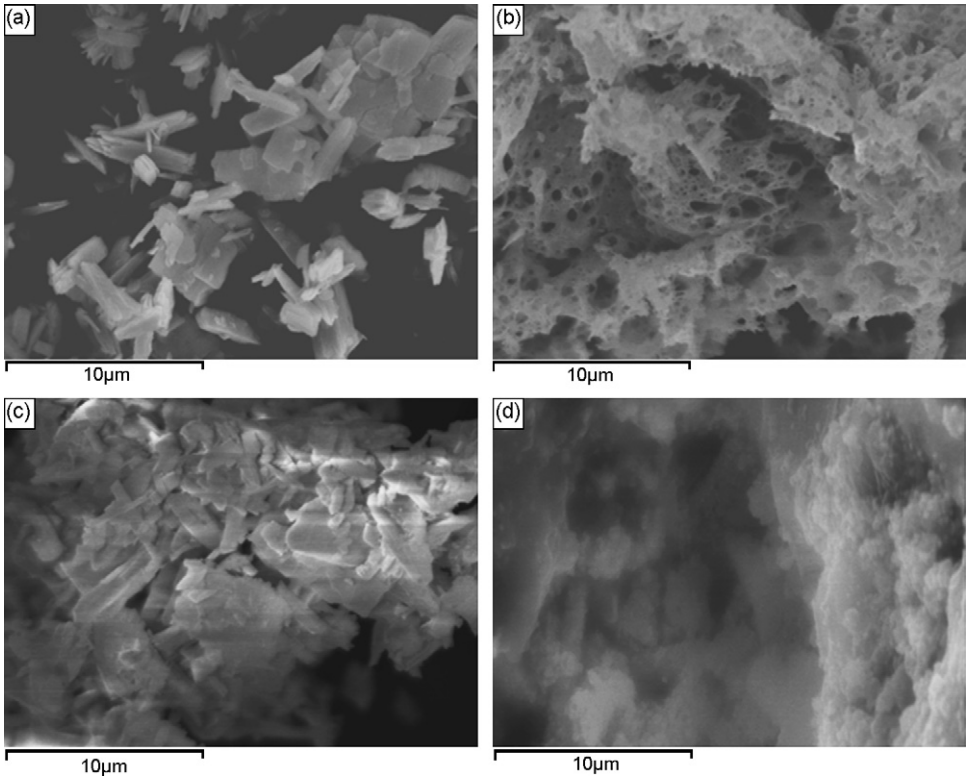

Fig. 5. SEM images of (a) SDC(OCP) powder, (b) SDC(GNP) powder, (c) SDC(OCP)-based composite and (d) SDC(GNP)-based composite.

weak bond between the foam SDC particles is broken. During fuel cell fabrication, the composite electrolyte can be pressed into a relative dense electrolyte layer, but it cannot reach full density because of the low sintering temperature. When the fuel cell is operated above the melting temperature of carbonates, the molten carbonates in the composite electrolyte will fill the interspaces between the SDC particles and form a dense composite electrolyte layer. In this case, more dense electrolyte layer can be obtained with the homogenous SDC(GNP)-based composite than with the aggregate SDC(OCP)-based composite. However, when the cell operating temperature is decreased to below such temperature, the molten carbonates begin to solidify, which will change the microstructure of the electrolyte layer. In this condition, the electrolyte layer will become less dense, especially for the homogenous SDC(GNP)-based composite. It is reflected by the fact that when tested at 400 °C the single cells with a SDC(GNP)-based composite electrolyte cannot provide stable OCV.

Derived from the *I–P* curves shown in Figs. 1–4, the maximum output power as a function of operating temperature for the four single cells is presented in Fig. 6. It can see that all cells exhibit excellent performances at intermediate temperatures, e.g. a maximum power density of 900 mW cm^{-2} or even higher value has been achieved at 600 °C for all cells. Even operated at 400 °C, the cell with a 0.3 mm thick SDC(OCP)-based composite electrolyte can offer a maximum power density as high as 310 mW cm^{-2}. These results are superior to the best performances ever reported for the ITFCs with a SDC or GDC thin-film electrolyte [1,15]. Such excellent performances can be attributed to the highly ionic conducting composite electrolyte and the compatible electrodes. In the case of the same composite electrolyte, the cells with a 0.3 mm thick electrolyte show higher output power than those with a 0.5 mm thick electrolyte at intermediate temperatures, resulting from the reduction of electrolyte resistance. It indicates that the cell performance can be further improved by reducing the thickness of the composite electrolyte layer and retaining its density to avoid gas crossover.

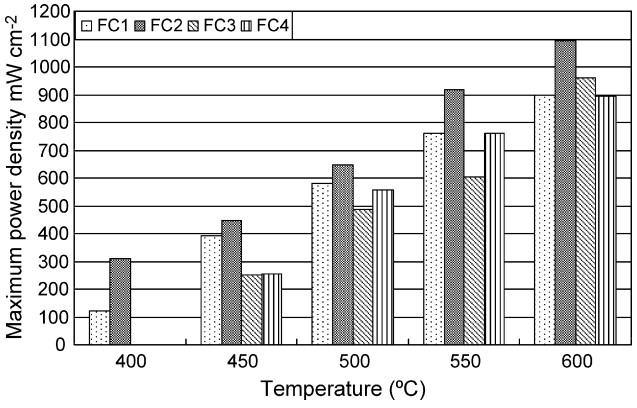

Fig. 6. The maximum power densities achieved at various temperatures for the four single cells. FC1, FC2, FC3 and FC4 represents the single cell with a 0.5 mm thick SDC(OCP)-based composite electrolyte, a 0.3 mm thick SDC(OCP)-based composite electrolyte, a 0.5 mm thick SDC(GNP)-based composite electrolyte, and a 0.3 mm thick SDC(GNP)-based composite electrolyte, respectively.

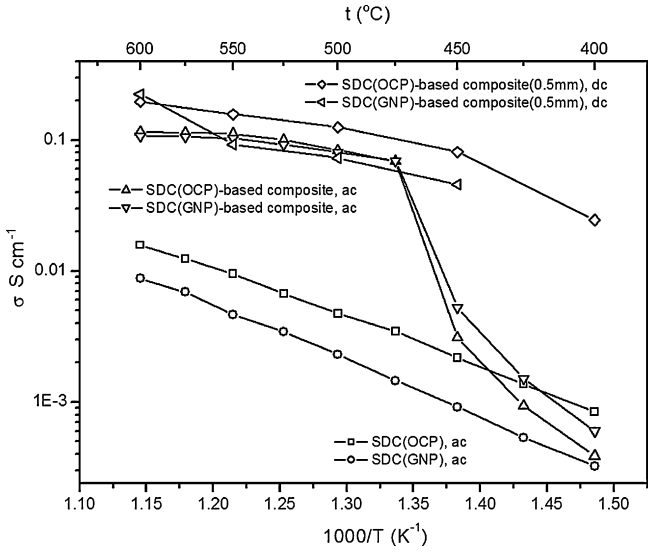

Fig. 7. Temperature dependence of the conductivities determined from both ac impedance spectroscopy and direct fuel cell *I–V* measurements for the SDC(OCP)-carbonate composite and the SDC(GNP)-carbonate composite. The *I–V* characteristics of the two cells with a 0.5 mm thick electrolyte are used to obtain the dc conductivity.

In the case of the same electrolyte thickness, the cells with a SDC(OCP)-based composite electrolyte are superior to those with a SDC(GNP)-based composite electrolyte at intermediate temperatures. It is obvious that the cell performance is influenced by the morphology of the SDC phase. This can be related to the difference in the conductivities of the SDC–carbonate composite electrolytes with different SDC phases. The dc conductivity of the fuel cell electrolyte can be obtained through direct measurements of the fuel cell *I–V* characteristics subtracting the influence of the electrodes and electrode/electrolyte interfaces as described by Zhu et al. [4]. According to the *I–V* characteristics shown in Figs. 1 and 2, the temperature dependence of the dc conductivities of the two composite electrolytes are determined and shown in Fig. 7. It is seen that the dc conductivity of the SDC(OCP)-based composite electrolyte are higher than that of the SDC(GNP)-based composite electrolyte at the temperature range of 400–600 °C, except at 600 °C.

For comparison, the ac conductivities of the two composite electrolytes and two pure SDC electrolytes obtained from the impedance spectroscopy are also shown in Fig. 7. In the ac conductivity curves, a sharp discontinuity is seen at 475 °C for both composite electrolytes. Such temperature is about 25 °C lower than the melting point of the Li_2CO_3–Na_2CO_3 eutectic, at which a superionic phase transition is assumed to occur [16]. Above that temperature both composite electrolytes show very high conductivities compared with the pure SDC electrolytes, and the conductivity of the SDC(OCP)-based composite electrolyte is slightly higher than that of the SDC(GNP)-based composite electrolyte, but below that temperature the conductivity of SDC(OCP)-based composite electrolyte is much lower than that of the SDC(GNP)-based composite electrolyte.

The SDC–carbonate composite is a two-phase material, which has been confirmed by the XRD results shown in Fig. 8.

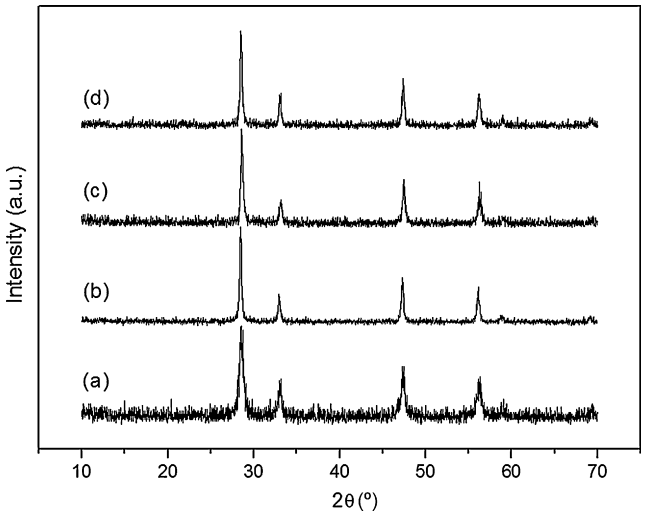

Fig. 8. XRD patterns of (a) SDC(OCP) powder, (b) SDC(GNP) powder, (c) SDC(OCP)-based composite and (d) SDC(GNP)-based composite.

In the composite, the SDC remains its own phase structure but the carbonates become amorphous. This reveals that there is a strong interaction between the SDC phase and the carbonate phase. It is expected that the defect (cationic vacancy) concentrations are much higher in the interfacial regions than in the bulk due to the formation of space charge zones in the interfacial regions. Therefore, more cations will accumulate in the interfacial regions. When a certain critical temperature is exceeded, the mobility of the cation in the interfacial regions enhances greatly due to the melting transition at sublattice level, thus a superionic conduction can be realized. Above that temperature, the carbonates begin to melt from sublattice to bulk with the increase of temperature, and all ions in molten carbonates are mobile. In this condition, the oxygen ion conduction in the SDC phase also contributes to the total conductivity, but the conductivity of the SDC phase is lower than that of the molten carbonate phase, leading to a slight difference in the conductivity of the two composite electrolytes. Below the transition temperature, the cations in the interface regions are not highly mobile because of the activation barrier, in the other hand, the oxygen ion conduction through the SDC phase is blocked by the dispersion of carbonate phases. The larger the size of SDC particle, the stronger the block effect of solid carbonate. Therefore, the SDC(OCP)-based composite electrolyte shows lower conductivity than the SDC(GNP)-based composite electrolyte.

According to Fig. 7, it is clear that the dc conductivity behaviors are not consistent with the ac conductivity behaviors, implying that the conduction mechanism of the composite electrolyte in fuel cell is different from that in air. In the H_2/air fuel cell, only the source ions, i.e. H^+ and O^{2-} can be conducted continuously and other ions, e.g. Li^+ and K^+ are blocked. As to the CO_3^{2-} ion, there is an argument that whether it can be conducted in the composite electrolyte during H_2/air fuel cell operation. Since there is a little content of CO_2 in air, the CO_3^{2-} ion can be conducted through the molten carbonate phase under the driving force of the CO_2 concentration. For both O^{2-} and CO_3^{2-} conductions, water is formed at the anode side of the fuel cell. But for H^+ conduction, water is formed at the cathode side. In this study, almost all water is observed at the flask and the tube connected to the cathodic gas outlet and hardly any water is observed at the flask and the tube connected to the anodic gas outlet when each cell is tested from 600 to 400 °C, indicating that proton is the main transport species. The proton conduction is assumed to occur through the cationic vacancy in the interfacial regions of the composite electrolyte. The CO_3^{2-} ion conduction is constrained by the transport of the smaller proton in the other direction. Since proton can be easily activated at low temperatures, the high dc conductivity of the composite electrolytes at IT range is expected. The difference in the proton conductivities of the SDC(OCP)-based composite and the SDC(GNP)-based composite may arise from the formation of consecutive interfacial regions between the two constituent phases.

4. Conclusion

ITFCs with a proton-conducting ceria–carbonate composite electrolyte and nickel-based electrodes are developed and excellent cell performances are achieved, which can be attributed to the highly proton-conducting composite electrolyte and the compatible electrodes. It is found that the cell performance is influenced by the SDC morphology and the electrolyte thickness. The proton conduction in the composite electrolyte is assumed to occur in the consecutive interfacial regions between the SDC phase and the carbonate phase. The unusual transport property, excellent cell performance and potential low cost make this kind of composite material a good candidate electrolyte for future cost-effective ITFCs.

Acknowledgements

This work was financially supported by the National Natural Science Foundation of China (Grant No. 20576063), National Basic Research Program of China (973 Program) (Grant No. 2007CB209706) and EC FP6 NANOCOFC (Nanocomposites for advanced fuel cell technology through EU-China and Turkey cooperation) project (Contract No. SSA 032308).

References

[1] Y.H. Zhang, X.Q. Huang, Z. Lu, Z.G. Liu, X.D. Ge, J.H. Xu, X.S. Xin, X.Q. Sha, W.H. Su, J. Power Sources 160 (2006) 1217–1220.
[2] J.W. Yan, H. Matsumoto, M. Enoki, T. Ishihara, Electrochem. Solid State Lett. 8 (2005) A389–A391.
[3] N. Ito, M. Iijima, K. Kimura, S. Iguchi, J. Power Sources 152 (2005) 200–203.
[4] B. Zhu, X.R. Liu, P. Zhou, J. Mater. Sci. Lett. 20 (2001) 591–594.
[5] G.Y. Meng, Q.X. Fu, S.W. Zha, C.R. Xia, X.Q. Liu, D.K. Peng, Solid State Ionics 148 (2002) 533–537.
[6] Q.X. Fu, W. Zhang, R.R. Peng, D.K. Peng, G.Y. Meng, B. Zhu, Mater. Lett. 53 (2002) 186–192.
[7] B. Zhu, J. Power Sources 114 (2003) 1–9.
[8] B. Zhu, X.T. Yang, J. Xu, Z.G. Zhu, S.J. Ji, M.T. Sun, J.C. Sun, J. Power Sources 118 (2003) 47–53.
[9] X.R. Liu, B. Zhu, J. Xu, J.C. Sun, Z.Q. Mao, Key Eng. Mater. 280–283 (2004) 425–430.

[10] J.D. Hu, S. Tosto, Z.X. Guo, Y.F. Wang, J. Power Sources 154 (2006) 106–114.
[11] J.B. Huang, Z.Q. Mao, L.Z. Yang, R.R. Peng, Electrochem. Solid State Lett. 8 (2005) A437–A440.
[12] J.B. Huang, L.Z. Yang, R.F. Gao, Z.Q. Mao, C. Wang, Electrochem. Commun. 8 (2006) 785–789.
[13] X.G. Zhang, M. Robertson, C. Deĉes-Petit, W. Qu, O. Kesler, R. Maric, D. Ghosh, J. Power Sources 164 (2007) 668–677.
[14] C.R. Xia, M.L. Liu, J. Am. Ceram. Soc. 84 (2001) 1903–1905.
[15] Q.L. Liu, K.A. Khor, S.H. Chan, J. Power Sources 161 (2006) 123–128.
[16] B. Zhu, M.D. Mat, Int. J. Electrochem. Sci. 1 (2006) 383–402.